JULY 07, 2020
CONFERENCE ONLINE
Graphene Online &2DM
Fundamental Research Insights
GO 2020

Composite super-moiré lattices in doubly-aligned graphene heterostructures

Zihao Wang1 [wangzihao205521@gmail.com] Supervisor: Konstantin Novoselov [Konstantin.Novoselov@manchester.ac.uk]

Zihao Wang, C. R. Woods[1,2], Yi Bo Wang[1], A. Knothe[2], Jun Yin[1], Yaping Yang[2], Lin Li[2], M. Hollwill[2], A. Mishchenko[1,2], A. K. Geim[1,2], Vladimir. I. Fal'ko[1,2], K. S. Novoselov*[1,2,3]*
[1]Department of Physics, University of Manchester, Oxford Road, Manchester, M13 9PL, UK
[2]National Graphene Institute, University of Manchester, Oxford Road, Manchester, M13 9PL, UK
[3]Department of Materials Science and Engineering, 9 Engineering Drive 1, Singapore

ABSTRACT

Van der Waals heterostructures, as vertical stacks assembled by different 2D crystals, have been widely used to produce combinations with predetermined functionalities. Apart from the selection and the sequence of 2D crystals, controlling the twist angle between stacking layers opened the use of another degree of freedom, especially for two crystals with similar lattice mismatch, which forms moire pattern. But this difference in the interatomic distances for the two crystals combined, determines the range in which the electronic spectrum is reconstructed, and thus is a barrier to the low energy regime. Here we present a way which allows spectrum reconstruction at all energies. By using graphene which is aligned simultaneously to two hexagonal boron nitride layers, one can make electrons scatter in the differential moiré pattern, which can have arbitrarily small wavevector and, thus results in spectrum reconstruction at arbitrarily low energies. We also demonstrate that the strength of such a potential relies crucially on the atomic reconstruction of graphene within the differential moiré super-cell.

Transport Measurement

If graphene is aligned with only one side hBN, a single moiré pattern is produced, and only one R_{XX} peak (secondary Dirac point) can be seen at concentrations corresponding to the periodicity of the moiré pattern [1].

Aligning graphene to both the top and the bottom hBN will produce two moiré patterns (green and red arrows mark them on both sides in Fig.1). At the same time, electrons can feel potential from both moiré patterns simultaneously, then second order processes can be allowed, which results in the reconstruction of the electronic spectrum at many other wavevectors (Blue arrows mark the corresponding peaks with periods labelled). Schematically, in Fig.2a, $\boldsymbol{b}_m{}^{\alpha}$ and $\boldsymbol{b}_k{}^{\beta}$ are the graphene-hBN moiré reciprocal lattice vectors. Their combination produces six new super-moiré patterns whose zone edge positions in carrier densities as a function of the angle between the second hBN layer and graphene are shown in Fig.2b for the case when the first hBN layer is held at zero angle mismatch (θ^{α} = 0) to graphene. For θ^{β} = 0.4°, the features correspond exactly to the observed peaks in R_{xx} and sign reversal of R_{xy}, thus revealing the presence of new generation Dirac points.

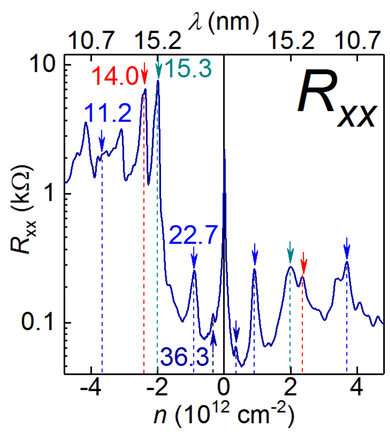

Fig.1:The Longitudinal resistance of doubly-aligned hBN/graphene/hBN device. *Rxx as a function of n for one of our devices with λ^{α} ≈ 15.3nm (φ_1 = 0°), λ^{β} ≈ 14.0nm (φ_2 = 0.4°). Lattice mismatch is taken as 1.64%. The moiré and super-moiré peaks are marked by arrows and also labelled with their periods(nm).*

To check that all these peaks indeed originate from the scattering on the additional periodic potentials (super-moiré) we measured the Brown-Zak oscillations at elevated temperatures. As the Fig.3 shows, most moiré periodicities have their corresponding fundamental frequencies [2].

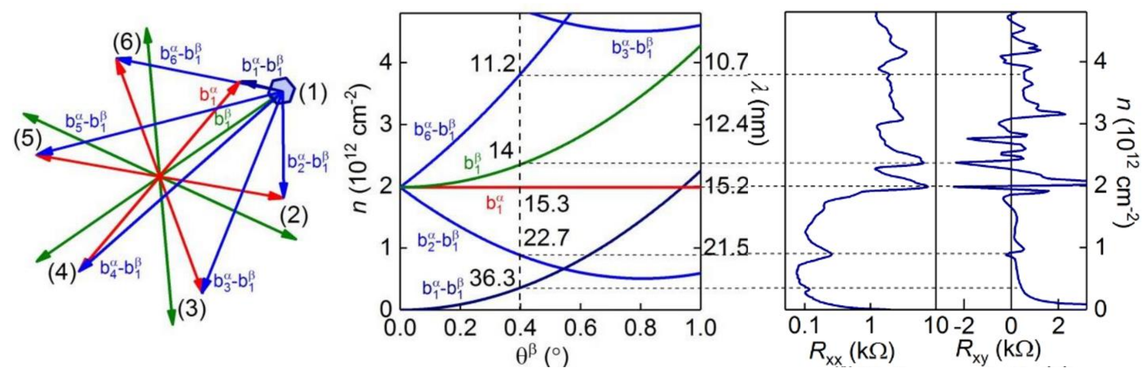

Fig.2: Super-moiré geometry. *a Reciprocal-space image of the area around graphene's K-point. $b_m{}^{\alpha}$ (green) and $b_m{}^{\beta}$ (red) for m = 1,2..6 are the graphene-hBN moiré reciprocal lattice vectors. $b_1{}^{\alpha} - b_m{}^{\beta}$ (blue) are the six super-moiré reciprocal lattice vectors. The blue hexagonal area indicates the $b_1{}^{\alpha} - b_1{}^{\beta}$ first Brillouin zone. b Carrier concentration of the first Brillouin zone edge for the two moiré and four lowest-energy super-moiré features as a function of θ^{β}(δ = 1.64%, θ^{α} = 0°). c Rxx peak and Rxy sign-changing positions in carrier concentration. Dashed lines connect values of carrier concentration for θ^{β}=0.4 in b to the position in c. Each line matches a peak and a corresponding changing sign.*

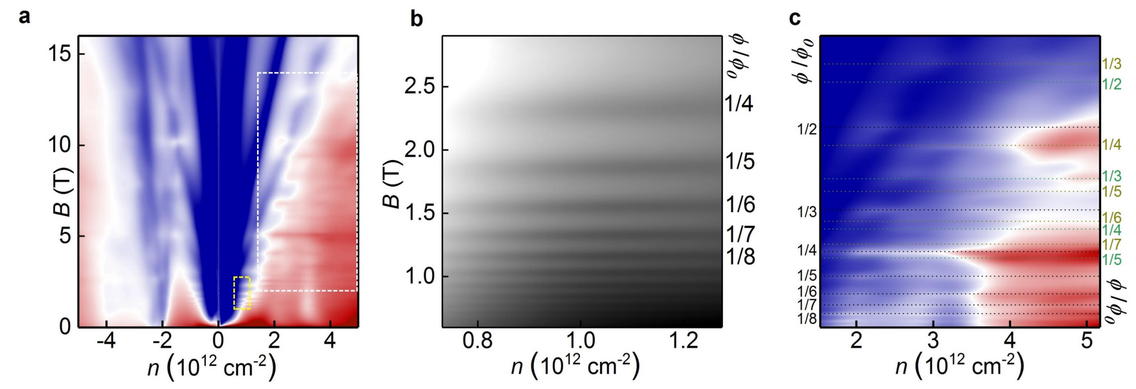

Fig.3: Brown-Zak oscillations at 70K. ***a*** *Map of σ_{xx}(n, B).* ***b*** *Zoom in into the low field part of the map, marked by yellow rectangle in (a), The Brown-Zak oscillations correspond to a moiré structure with periodicity of 22.7nm and the fundamental field is 9.3T.* ***c*** *Zoom in into the high field part of the map, marked by white rectangle in (a). The Brown-Zak oscillations corresponding to a moiré structures of different periodicities are marked by dashed lines of different colours. Black - 15.3nm (BF=20.5T), green 14.0nm (BF=24.2T) and brown – 11.2nm (BF=38T).*

AFM Image

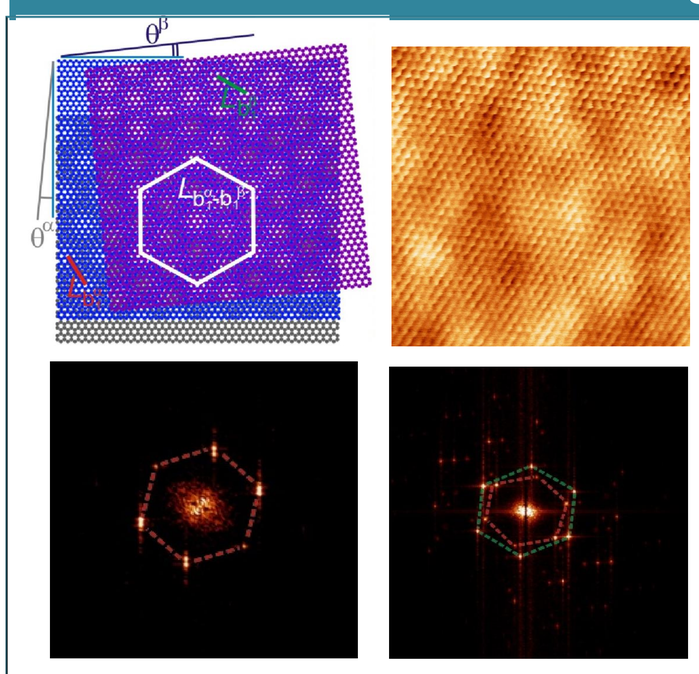

The transfer procedures have been previously described in [3] with the exception that not only the bottom but also the top hBN is aligned to the graphene. **The Fourier transformation of AFM image, c and d, before and after bringing the hBN/graphene single aligned heterostructure into contact with the second thin hBN proves the double alignment clearly.**

Fig.4: AFM Characterisation. ***a*** *Illustration of the two individual moiré patterns and super-moiré pattern with three overlapping hexagonal lattices.* ***b*** *AFM image of the moiré patterns of doubly-aligned devices* ***c*** *Fourier transformation of the image of the single hBN/graphene heterostructure before aligning to the second thin hBN-layer* ***d*** *Fourier transformation of the image in* ***b****, showing two sets of distinct hexagonal patterns (red and green dashed hexagons).*

Raman Broadening

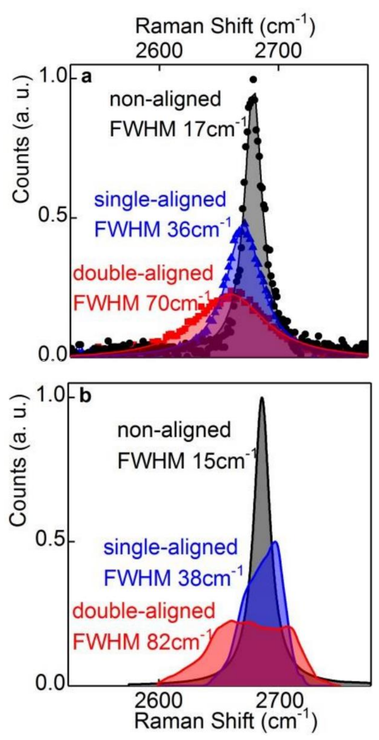

Previous work[4] has identified that the perfectly aligned hBN/graphene crystals form a commensurate state which relies upon strain, modulating with the moiré pattern to minimise stacking-dependent van der Waals adhesion and elastic energy of graphene. **Here for double algined samples, the FWHM of doubly aligned samples doubled. If two hBN layers are treated independently, the signature in the Raman spectrum would remain unchanged. We attribute this change to restructuring of strain within the supermoire unit cells. This observation supports that the two moires mix through strain field which should have periodicities following not only moires but also supermoires.**

Fig. 5: Strain distribution in the aligned graphene-hBN heterostructures. *Raman spectra (2D-peak region) for an unaligned sample (grey), single-aligned sample (blue), and double-aligned sample (red). (a) Experimental results. (b) Molecular dynamics relaxation simulations.*

CONCLUSION

Through the above analysis of transport measurement, AFM and Raman characterization, the conclusion can be drawn that graphene's electronic spectrum is significantly altered by scattering from super-moiré structures described by the pre-existing moiré between graphene and its substrate and encapsulating hBN layers. These alterations may be considered in two ways; as double scattering events from both graphene-hBN moiré patterns, or as single scattering events from a reconstructed graphene layer. Such super-moiré potential can be of arbitrarily small wavevector (unlike moiré potential from single hBN aligned with graphene), which allows modification of the graphene band structure at arbitrarily low energies.

REFERENCES

[1] M.Yankowitz et al., Emergence of superlattice Dirac points in graphene on hexagonal boron nitride. Nat. Phys. 8, 382-386 (2012). [2] R. K. Kumar et al., High-temperature quantum oscillations caused by recurring Bloch states in graphene superlattices. Science 357, 181-184 (2017). [3] T. Uwanno et al., Fully dry PMMA transfer of graphene onh-BN using a heating/cooling system. 2D Materials 2, 041002 (2015). [4] C.R. Woods et al., Commensurate-incommensurate transition in graphene on hexagonal boron nitride. Nat. Phys. 10, 451-456 (2014).